

Comparative Analysis Of Variations In The Slant Range And Free Space Path Loss For Sun-Synchronous Satellite Operating At K, Ku And Ka Frequency Bands

Olisa Joseph Otunuya¹

Department / Office of National Space Research and Development Agency, (NASRDA),
Abuja, Nigeria
jossilee86@gmail.com

Precious, Diepiriye Henry²

Department / Office of National Space Research and Development Agency (NASRDA),
Abuja, Nigeria
henriresh50@gmail.com

Ogunrombi, Tijesuni Samson³

Department / Office of National Space Research and Development Agency, (NASRDA),
Abuja, Nigeria
tijesunisamson@yahoo.com

Abstract— In this paper, comparative analysis of variations in the slant range and free space pathloss for sun-synchronous satellite-earth communication link operating at K, Ku and Ka frequency bands is presented. The case study satellite is NIGERIASAT 2 which is a Sun-Synchronous Orbit (SSO) satellite with orbital altitude of 718 km, perigee of 686.4 km, apogee of 700.3 km, orbital inclination of 97.8 °, orbital period of 98.5 minutes and semi major axis of 7064 km. The elevation angles extracted from 10-days online satellite tracking data for NIGERIASAT 2 (Available at <https://www.n2yo.com/passes/?s=37789>) with earth station in Akwa Ibom State Nigeria at latitude of 5.015209° and longitude of 7.912815° are used in the analysis. The results show that the graph of the elevation angle has a shape that repeats every 60 hours. Also, the minimum elevation angle is 10° while the maximum elevation angle is 88° which occurred once at the 144th hour. Also, the lowest slant range of 700.38 km occurred at the 144th hour with the highest elevation angle of 88° while the highest slant range of 2,155.28 km occurred at 228th hour with the lowest elevation angle of 10°. The results show that among the three frequency bands, the Ka-band with frequency of 35 GHz has the highest path loss in all the elevation angles. In the other hand, the 15 GHz Ku-band frequency has the lowest pathloss among the three frequencies considered.

1. Introduction

Satellite communication systems generally operate wirelessly in the microwave frequency band [1,2,3,4,5,6,7,8,9,10]. Notably, microwave signals require line-of-sight and this is generally adopted in satellite communication systems. However, even with clear line of sight, the satellite signal still suffer from free space path loss. Besides, there are other atmospheric and interference issues that can also affect the satellite signal [8, 9, 10, 11, 12, 13, 14, 15, 16, 17, 18, 19, 20, 21, 22, 23]. In many cases, the effect on the signal is dependent on the frequency of the signal as well as the propagation path length. The degree to which signal is effected also depends on the type of satellite and the satellite orbit. In this paper, the focus is on the Sun-synchronous satellite which is mainly used for Earth observation purposes [24,25,26,27,28,29].

Sun-synchronous satellite or Sun-Synchronous Orbit (SSO) satellite is one of the categories of satellite which is designed and located in orbit in such a way that it synchronises its position and movements relative to the sun [30,31,32,33,34,35]. Generally, the Sun-

Keywords— Free Space Pathloss, Sun-Synchronous Satellite, NIGERIASAT 2, Slant Range, Communication Link

synchronous satellite is a form of polar satellite and their orbit fall within the low orbit and medium orbit with orbit height in the range of 200 to 1000 km [36,37,38,39,40].

Applications of sun-synchronous satellite in the communication industry require accurate computation of some key parameters, among which include the slant range, inclination angle, elevation angle, propagation loss, visibility, among others. In this paper, the focus is on the slant range and propagation loss based on the free space path loss model. Notably, the slant range is dependent on the position coordinates of the satellite relative to the earth station. On the other hand path loss is dependent on the slant range and the operating frequency. In this paper, the variation of the slant range and free space path loss of NIGERIASAT 2 sun-synchronous satellite relative to a given earth location is studied [41,42,43,44,45]. The study examined the variation of the two parameters as the case

study satellite makes a round trip along its orbit. The study also considered the variation of the pathloss for the following microwave frequency bands, namely; K, Ku and Ka frequency bands.

2. Methodology

The focus in this paper is to evaluate the variations in the slant range and the free space path loss for a sun-synchronous satellite-earth communication link. If the elevation angle, θ_e of a satellite communication link is known, then the slant range and the path loss can be determined. The image used for the explanation of the mathematical expressions used for the determination of the slant range, L_s based on the elevation angle, θ_e is given in Figure 1. In Figure 1, P is the subsatellite point, R_e is the earth radius (6378 km), satellite orbital altitude (H_s) of 718 km and L_s is the slant range which is required to compute the free space pathloss.

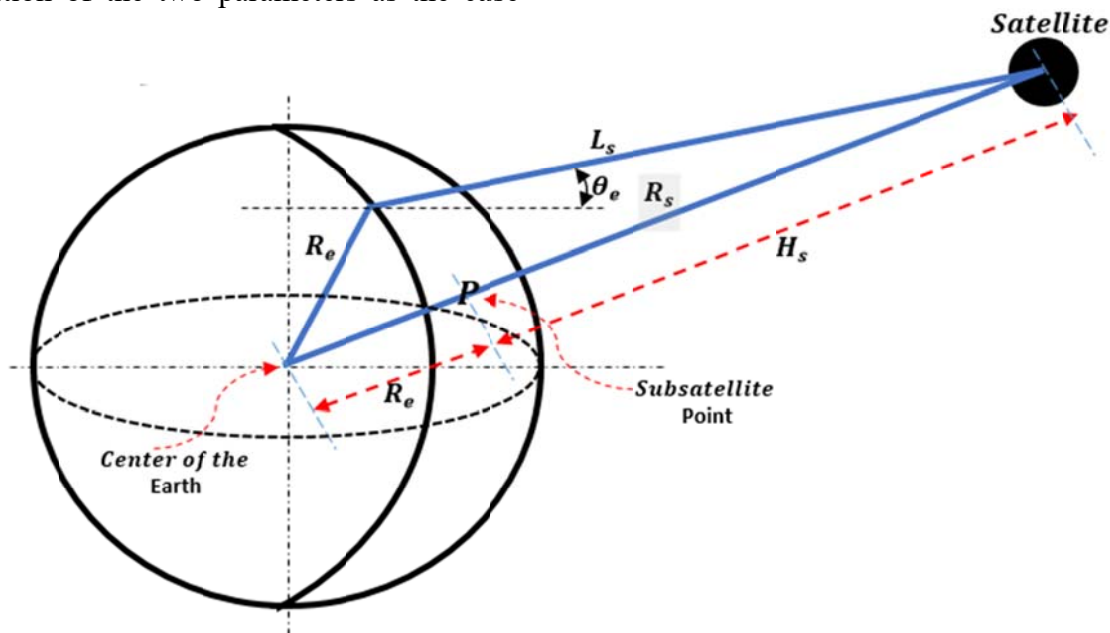


Figure 1 The image used for the explanation of the mathematical expressions used for the determination of the slant range, L_s based on the elevation angle, θ_e

The orbital radius (R_s) of the satellite is given as;

$$R_s = R_e + H_s \quad (1)$$

Cosine law can then be applied to give

$$R_s^2 = R_e^2 + L_s^2 - 2(R_e)(L_s) \cos(90 - \theta_e) \quad (2)$$

Hence,

$$L_s = R_e \left[\sqrt{\left(\left(\frac{R_s}{R_e}\right)^2 - \cos^2(\theta_e)\right)} - \sin(\theta_e) \right] \quad (3)$$

$$L_s = R_e \left[\sqrt{\left(\left(\frac{R_e + H_s}{R_e}\right)^2 - \cos^2(\theta_e)\right)} - \sin(\theta_e) \right] \quad (4)$$

Therefore, pathloss $FSPL$ is given as,

$$FSPL = 20\log(L_s) + 20\log(f) + 92.45 \quad (5)$$

Where f is the frequency expressed in MHz while L_s is expressed in Km

The case study satellite in this paper is NIGERIASAT 2. NIGERIASAT 2 is a Nigerian Sun-synchronous orbit (SSO) satellite with

orbital altitude of 718 km, perigee of 686.4 km, apogee of 700.3 km, orbital inclination of 97.8°, orbital period of 98.5 minutes and semi major axis of 7064 km. The elevation angle extracted from 10-days online satellite tracking data for

NIGERIASAT 2 (Available at <https://www.n2yo.com/passes/?s=37789>) with earth station in Akwa Ibom State Nigeria at latitude of 5.015209° and longitude of 7.912815° is presented in Table 1.

Table 1 The elevation angle extracted from 10-days online satellite tracking data for NIGERIASAT 2 (Available at <https://www.n2yo.com/passes/?s=37789>) with earth station in Akwa Ibom State Nigeria at latitude of 5.015209° and longitude of 7.912815°

S/N	Time (Hour)	Elevation Angle (°)	S/N	Time (Hour)	Elevation Angle (°)	S/N	Time (Hour)	Elevation Angle (°)
1	0.0000	33	11	84.5333	79	21	169.1500	27
2	1.6500	11	12	96.8833	43	22	179.8000	20
3	12.2667	47	13	107.5500	12	23	181.4333	20
4	24.6167	74	14	109.1667	31	24	192.1500	46
5	36.9000	52	15	119.9000	28	25	204.4167	66
6	47.6500	17	16	121.5333	14	26	216.7833	52
7	49.2667	22	17	132.1667	39	27	227.4500	10
8	59.9000	24	18	144.5167	88		Minimum	10
9	61.5333	17	19	156.7833	63		Maximum	88
10	72.2667	55	20	167.5500	15		Average	49
							Δ%	±79.591836

3. Results and Discussion

The earth radius (6378 km), satellite orbital altitude (Hs) of 718 km and elevation angle data in Table 1 are used to compute the slant range and free space pathloss for 15 GHz Ku-band, 25

GHz K-band and 35 GHz Ka-band frequencies and the results are presented in Table 2 and in Figure 2 to Figure 7.

Table 2 The results of the computed slant range and free space pathloss for 15 GHz Ku-band, 25 GHz K-band and 35 GHz Ka-band frequencies

Time (Hour)	Elevation Angle (°)	Slant range, L (Km)	Pathloss for 15 GHz Ku-Band	Pathloss for 25 GHz K-Band	Pathloss for 35 GHz Ka-Band
0	33	1,161.58	177.2628	181.6998	184.6223
1.65	11	2,084.58	182.3422	186.7792	189.7017
12.2667	47	919.10	175.2291	179.6661	182.5887
24.6167	74	725.27	173.1718	177.6088	180.5314
36.9	52	862.97	174.6818	179.1187	182.0413
47.65	17	1,726.43	180.7048	185.1418	188.0643
49.2667	22	1,500.19	179.4848	183.9218	186.8443
59.9	24	1,424.41	179.0345	183.4715	186.394
61.5333	17	1,726.43	180.7048	185.1418	188.0643
72.2667	55	834.75	174.393	178.8299	181.7525
84.5333	79	711.77	173.0087	177.4456	180.3682

96.8833	43	973.73	175.7306	180.1676	183.0902
107.55	12	2,017.25	182.057	186.494	189.4165
109.1667	31	1,210.63	177.622	182.059	184.9816
119.9	28	1,293.48	178.197	182.634	185.5566
121.5333	14	1,892.14	181.5009	185.9379	188.8604
132.1667	39	1,038.90	176.2933	180.7303	183.6528
144.5167	88	700.38	172.8686	177.3055	180.2281
156.7833	63	775.79	173.7567	178.1937	181.1162
167.55	15	1,834.11	181.2303	185.6673	188.5899
169.15	27	1,323.86	178.3987	182.8357	185.7582
179.8	20	1,583.93	179.9566	184.3935	187.3161
181.4333	20	1,583.93	179.9566	184.3935	187.3161
192.15	46	931.88	175.349	179.786	182.7085
204.4167	66	758.87	173.5652	178.0022	180.9248
216.7833	52	862.97	174.6818	179.1187	182.0413
227.45	10	2,155.28	182.6319	187.0689	189.9914
Minimum	10.00	700.38	172.87	177.31	180.23
Maximum	88.00	2,155.28	182.63	187.07	189.99
Average	49	1427.832	177.7502	182.1872	185.1098
$\Delta\%$	± 79.591836	± 50.947688	± 2.7463649	± 2.6794801	± 2.6371758

The graph of elevation angle versus the time (in hours) within the 10-days online satellite tracking data for NIGERIASAT 2 is shown in Figure 2 while the graph of slant range versus the time (in hours) is shown in Figure 3. The results show that the graph of the elevation angle has a shape that repeats every 60 hours. Also, the minimum elevation angle is 10° while the maximum elevation angle is 88° which occurred once at the 144th hour.

On the other hand, from Figure 3 and Figure 2, the results show that the slant range is high at the low elevation angles and low at the high elevation angles. Specifically, the lowest slant range of 700.38 km occurred at the 144th hour with the highest elevation angle of 88° while the highest slant range of 2,155.28 km occurred at 228th hour with the lowest elevation angle of 10° . The graph of slant range versus elevation

angle obtained within the 10-days online satellite tracking data for NIGERIASAT 2 is shown in Figure 4. The results show that the slant range is highest at the lowest elevation angle of 10° and lowest at the highest elevation angle of 88° .

The graph of pathloss versus the time (in hours) within the 10-days online satellite tracking data for NIGERIASAT 2 is shown in Figure 5, that of pathloss versus elevation angle is shown in Figure 6 while that of pathloss versus slant range is shown in Figure 7. The results show that among the three frequency bands, the Ka-band with frequency of 35 GHz has the highest path loss in all the elevation angles. The 15 GHz Ku-band frequency has the lowest pathloss among the three frequencies considered. Also, the pathloss for each of the frequencies is highest at the lowest elevation angle of 10° and lowest at the highest elevation angle of 88° .

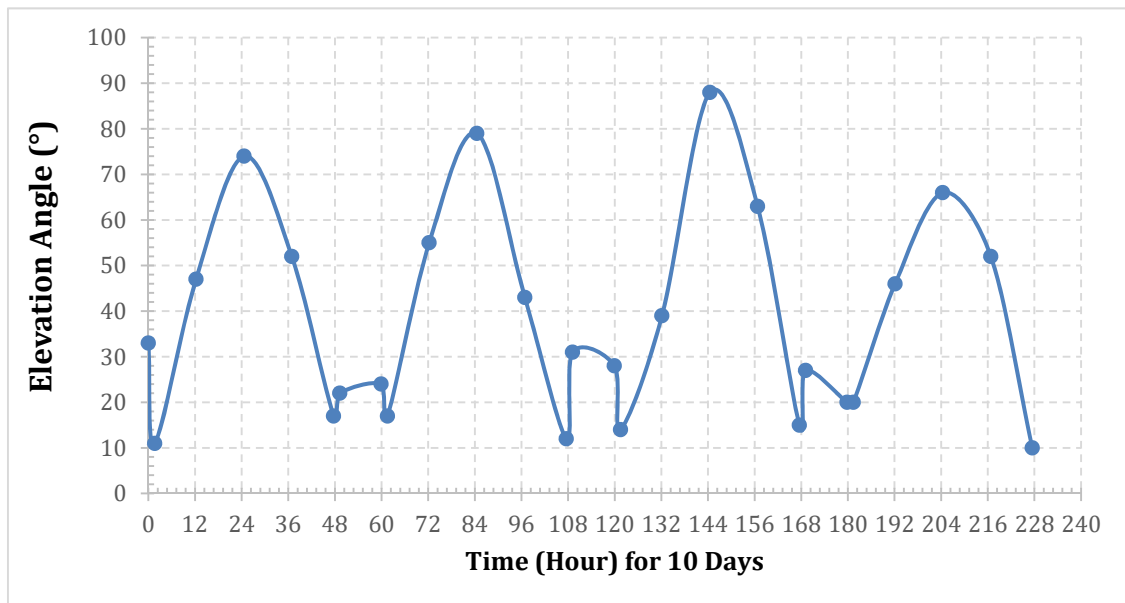


Figure 2 The graph of elevation angle versus the time (in hours) within the 10-days online satellite tracking data for NIGERIASAT 2 (Available at <https://www.n2yo.com/passes/?s=37789>)

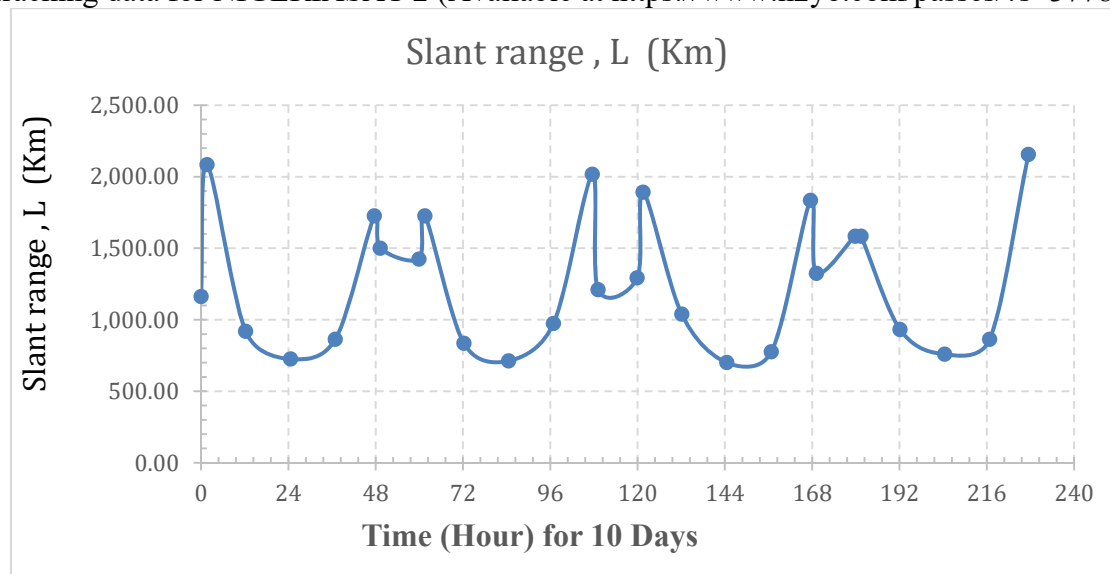


Figure 3 The graph of slant range versus the time (in hours) within the 10-days online satellite tracking data for NIGERIASAT 2 (Available at <https://www.n2yo.com/passes/?s=37789>)

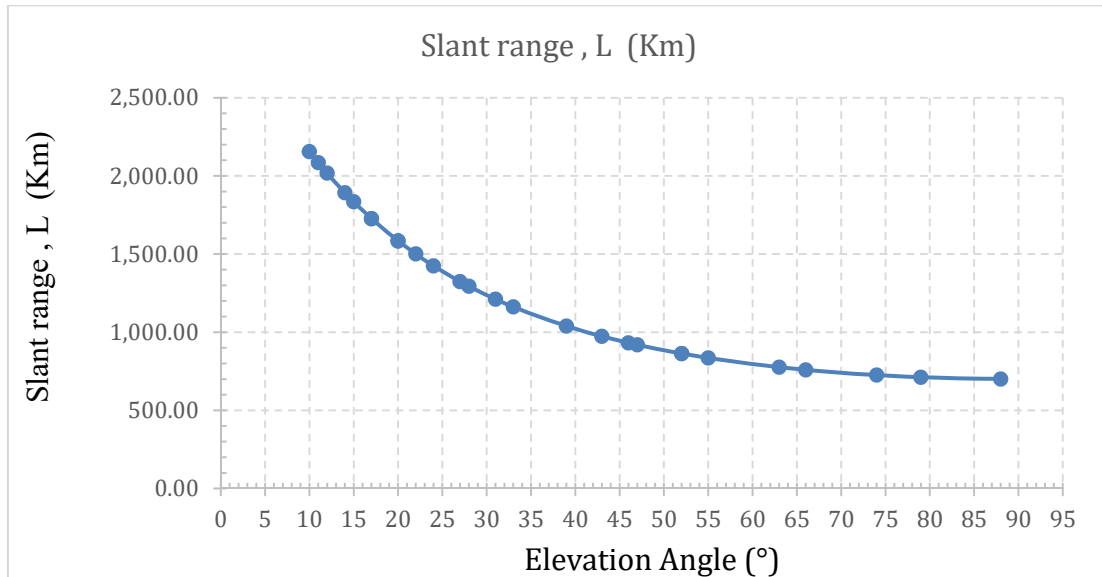


Figure 4 The graph of slant range versus elevation angle obtained within the 10-days online satellite tracking data for NIGERIASAT 2 (Available at <https://www.n2yo.com/passes/?s=37789>)

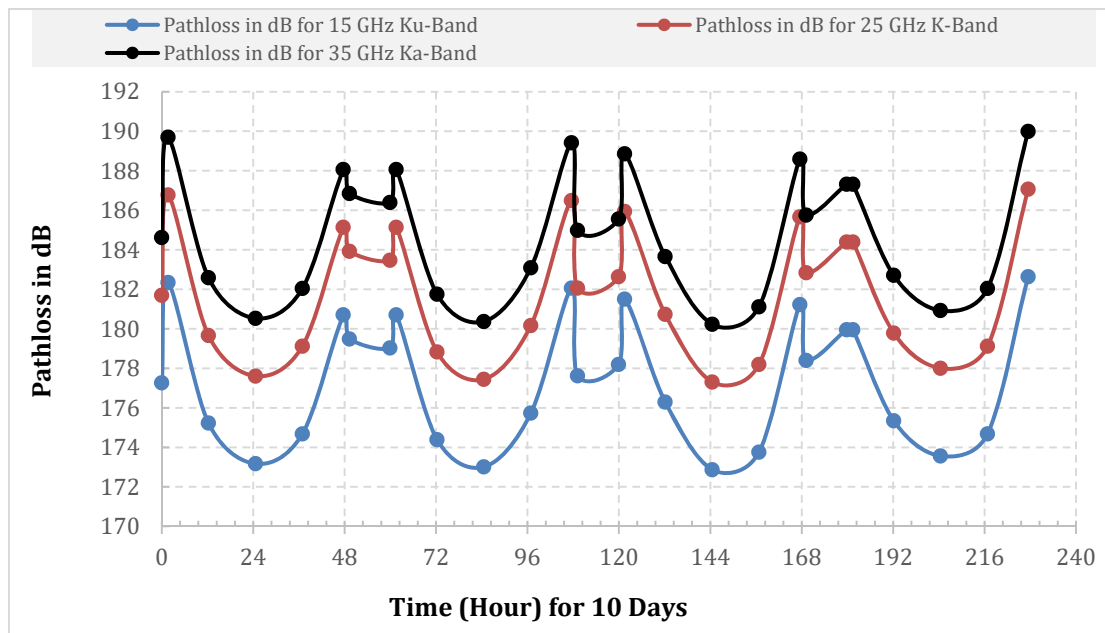


Figure 5 The graph of pathloss versus the time (in hours) within the 10-days online satellite tracking data for NIGERIASAT 2 (Available at <https://www.n2yo.com/passes/?s=37789>)

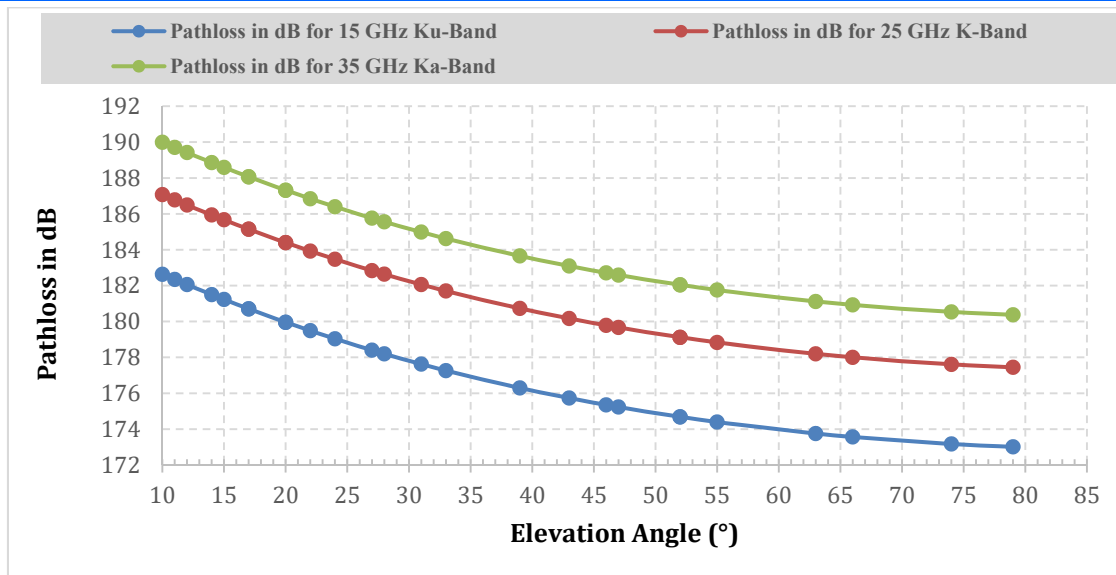


Figure 6 The graph of pathloss versus elevation angle obtained within the 10-days online satellite tracking data for NIGERIASAT 2 (Available at <https://www.n2yo.com/passes/?s=37789>)

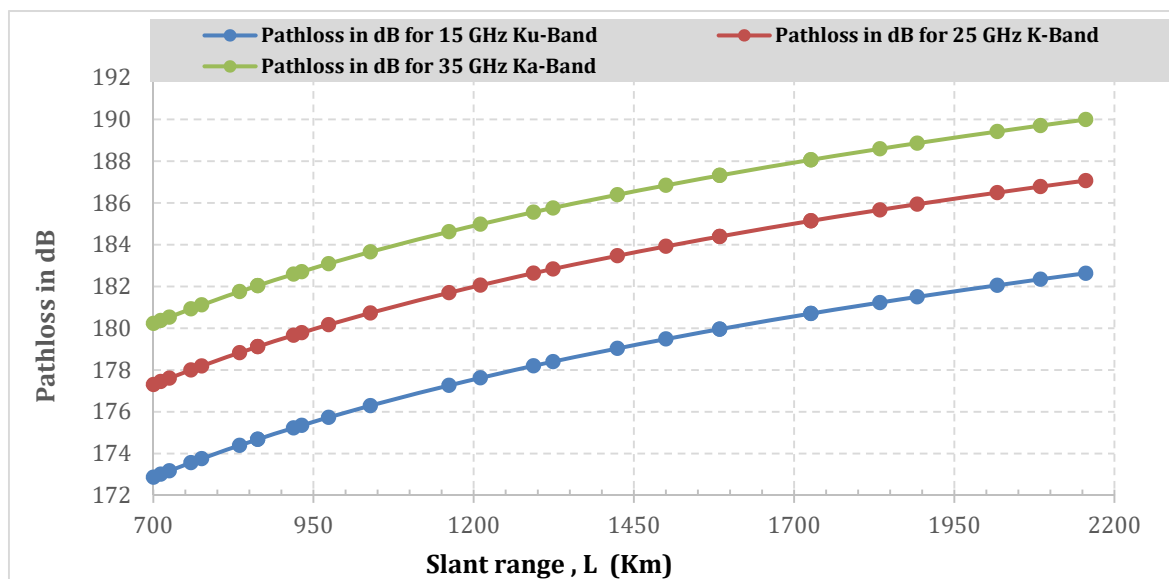


Figure 4 The graph of pathloss versus slant range obtained within the 10-days online satellite tracking data for NIGERIASAT 2 (Available at <https://www.n2yo.com/passes/?s=37789>)

Conclusion

The slant range and pathloss of a sun-synchronous satellite is studied. The study considered the pathloss for three different frequency bands, namely; the Ku-band, the K-band and the Ka-band. The values of the elevation angle of the satellite are obtained from a 10-days satellite track prediction data obtained using an online tool available at <https://www.n2yo.com/passes/?s=37789>. The elevation angle are then used to determine the slant range and pathloss for the selected frequency bands. The results showed that among the three frequency bands considered in the study, the Ka-band with the highest frequency

has the highest pathloss in all cases. Also, the elevation angle, the slant range and the pathloss of the satellite vary over a period of time and repeats the values periodically.

References

1. Wells, J. (2009). Faster than fiber: The future of multi-G/s wireless. *IEEE microwave magazine*, 10(3), 104-112.
2. Sharma, A., & Singh, G. (2009). Rectangular microstrip patch antenna design at THz frequency for short distance wireless communication systems. *Journal of Infrared, Millimeter, and Terahertz Waves*, 30(1), 1-7.
3. Meng, Y. S., & Lee, Y. H. (2010). Investigations of foliage effect on modern wireless

- communication systems: A review. *Progress In Electromagnetics Research*, 105, 313-332.
4. Simeon, Ozuomba (2014) "Fixed Point Iteration Computation Of Nominal Mean Motion And Semi Major Axis Of Artificial Satellite Orbiting An Oblate Earth." *Journal of Multidisciplinary Engineering Science and Technology (JMEST)* Vol. 1 Issue 4, November – 2014 . Available at: <http://www.jmest.org/wp-content/uploads/JMESTN42353750.pdf>
 5. Sharma, A., Khare, K., & Shrivastava, S. C. (2016). Dielectric resonator antenna for X band microwave application. *Research & Reviews, International Journal of Advanced Research in Electrical, Electronics and Instrumentation Engineering*.
 6. Ullah, S., Ahmad, S., Khan, B. A., Tahir, F. A., & Flint, J. A. (2019). An hp-shape hexa-band antenna for multi-standard wireless communication systems. *Wireless Networks*, 25(3), 1361-1369.
 7. Anwer, M. S., & Guy, C. (2014). A survey of VANET technologies. *Journal of Emerging Trends in Computing and Information Sciences*, 5(9), 661-671.
 8. Anwer, M. S., & Guy, C. (2014). A survey of VANET technologies. *Journal of Emerging Trends in Computing and Information Sciences*, 5(9), 661-671.
 9. Simeon, Ozuomba. (2016) "Comparative Analysis Of Rain Attenuation In Satellite Communication Link For Different Polarization Options." *Journal of Multidisciplinary Engineering Science and Technology (JMEST)* Vol. 3 Issue 6, June – 2016. Available at: <http://www.jmest.org/wp-content/uploads/JMESTN42353755.pdf>
 10. Waterhouse, R., & Novack, D. (2015). Realizing 5G: Microwave photonics for 5G mobile wireless systems. *IEEE Microwave Magazine*, 16(8), 84-92.
 11. Su, Y., Liu, Y., Zhou, Y., Yuan, J., Cao, H., & Shi, J. (2019). Broadband LEO satellite communications: Architectures and key technologies. *IEEE Wireless Communications*, 26(2), 55-61.
 12. Simeon, Ozuomba. (2017). "Determination Of The Clear Sky Composite Carrier To Noise Ratio For Ku-Band Digital Video Satellite Link" *Science and Technology Publishing (SCI & TECH)* Vol. 1 Issue 7, July – 2017. Available at: <http://www.scitechpub.org/wp-content/uploads/2021/03/SCITECHP420150.pdf>
 13. Kyrgiazos, A., Evans, B., Thompson, P., Mathiopoulos, P. T., & Papaharalabos, S. (2014). A terabit/second satellite system for European broadband access: a feasibility study. *International Journal of Satellite Communications and Networking*, 32(2), 63-92.
 14. Kalu, C., Ozuomba, S., & Udofia, K. (2015). WEB-BASED MAP MASHUP APPLICATION FOR PARTICIPATORY WIRELESS NETWORK SIGNAL STRENGTH MAPPING AND CUSTOMER SUPPORT SERVICES. *European Journal of Engineering and Technology* Vol, 3(8).
 15. Ioannides, R. T., Pany, T., & Gibbons, G. (2016). Known vulnerabilities of global navigation satellite systems, status, and potential mitigation techniques. *Proceedings of the IEEE*, 104(6), 1174-1194.
 16. Ozuomba, S., Kalu, C., & Obot, A. B. (2016). Comparative Analysis of the ITU Multipath Fade Depth Models for Microwave Link Design in the C, Ku, and Ka-Bands. *Mathematical and Software Engineering*, 2(1), 1-8.
 17. Samuel, W., Ozuomba, S., & Constance, K. (2019). Self-Organizing Map (SOM) Clustering of 868 MHz Wireless Sensor Network Nodes Based on Egli Pathloss Model Computed Received Signal Strength. *NETWORK*, 6(12).
 18. Bernardo, N., Watanabe, F., Rodrigues, T., & Alcântara, E. (2017). Atmospheric correction issues for retrieving total suspended matter concentrations in inland waters using OLI/Landsat-8 image. *Advances in Space Research*, 59(9), 2335-2348.
 19. Ozuomba, S., Johnson, E., & Rosemary, N. C. (2018). Characterisation of Propagation Loss for a 3G Cellular Network in a Crowded Market Area Using CCIR Model. *Review of Computer Engineering Research*, 5(2), 49-56.
 20. Weissman, D. E., Stiles, B. W., Hristova-Veleva, S. M., Long, D. G., Smith, D. K., Hilburn, K. A., & Jones, W. L. (2012). Challenges to satellite sensors of ocean winds: Addressing precipitation effects. *Journal of Atmospheric and Oceanic Technology*, 29(3), 356-374.
 21. Samuel, W., Ozuomba, S., & Asuquo, P. M. (2019). EVALUATION OF WIRELESS SENSOR NETWORK CLUSTER HEAD SELECTION FOR DIFFERENT PROPAGATION ENVIRONMENTS BASED ON LEE PATH LOSS MODEL AND K-MEANS ALGORITHM. *EVALUATION*, 3(11).
 22. Su, Y., Liu, Y., Zhou, Y., Yuan, J., Cao, H., & Shi, J. (2019). Broadband LEO satellite communications: Architectures and key technologies. *IEEE Wireless Communications*, 26(2), 55-61.
 23. Ozuomba, S., Johnson, E. H., & Udoiwod, E. N. (2018). Application of Weissberger Model for Characterizing the Propagation Loss in a *Gliricidia sepium* Arboretum. *Universal Journal of Communications and Network*, 6(2), 18-23.
 24. Eleveld, M. A., Van der Wal, D., & Van Kessel, T. (2014). Estuarine suspended particulate

- matter concentrations from sun-synchronous satellite remote sensing: Tidal and meteorological effects and biases. *Remote sensing of environment*, 143, 204-215.
25. Khamseh, H. B., & Navabi, M. (2011). On reduction of longest accessibility gap in LEO sun-synchronous satellite missions. *Journal of Aerospace Technology and Management*, 3(1), 53-58.
 26. Tomita, H., & Kubota, M. (2011). Sampling error of daily mean surface wind speed and air specific humidity due to Sun-synchronous satellite sampling and its reduction by multi-satellite sampling. *International journal of remote sensing*, 32(12), 3389-3404.
 27. Mei, P., Weiwei, W., Jing, W., & Ming, L. (2011). Study on attenuation factor of Si solar array for satellite in sun synchronous orbit. *Spacecraft Engineering*, 20(5), 61-67.
 28. Tian, T., Zong, Q., Chang, Z., Wang, Y., & Yang, X. (2016). Statistical analysis of one Chinese sun-synchronous satellite anomalies. *Science China Technological Sciences*, 59(4), 540-546.
 29. Farrahi, A., & Pérez-Grande, I. (2017). Simplified analysis of the thermal behavior of a spinning satellite flying over Sun-synchronous orbits. *Applied Thermal Engineering*, 125, 1146-1156.
 30. Paek, S. W., Kim, S., Kronig, L., & de Weck, O. (2020). Sun-synchronous repeat ground tracks and other useful orbits for future space missions. *The Aeronautical Journal*, 124(1276), 917-939.
 31. Castronuovo, M. M. (2011). Active space debris removal—A preliminary mission analysis and design. *Acta Astronautica*, 69(9-10), 848-859.
 32. Paek, S. W., & Kim, S. (2018). Space-based Earth remote sensing: Part 1. Satellite orbit theory. *Satellite Oceanography and Meteorology*, 3(1).
 33. Legge Jr, R. S. (2014). *Optimization and valuation of reconfigurable satellite constellations under uncertainty* (Doctoral dissertation, Massachusetts Institute of Technology).
 34. Richard, M., Kronig, L. G., Belloni, F., Gass, V., Araromi, O. A., Shea, H., ... & Thiran, J. P. (2013). Uncooperative rendezvous and docking for MicroSats. In *6th International Conference on Recent Advances in Space Technologies, RAST 2013* (No. CONF).
 35. Sarda, K., CaJacob, D., Orr, N., & Zee, R. (2018). Making the invisible visible: precision RF-emitter geolocation from space by the hawkeye 360 pathfinder mission.
 36. Mason, J., Stupl, J., Marshall, W., & Levit, C. (2011). Orbital debris–debris collision avoidance. *Advances in Space Research*, 48(10), 1643-1655.
 37. Matar, J., Rodriguez-Cassola, M., Krieger, G., López-Dekker, P., & Moreira, A. (2019). MEO SAR: System concepts and analysis. *IEEE Transactions on Geoscience and Remote Sensing*, 58(2), 1313-1324.
 38. Georgescu, A., Gheorghe, A. V., Piso, M. I., & Katina, P. F. (2019). Critical space infrastructures. In *Critical Space Infrastructures* (pp. 21-36). Springer, Cham.
 39. Schlüssel, P., & Kayal, G. (2017, September). Introduction to the next generation EUMETSAT Polar System (EPS-SG) observation missions. In *Sensors, Systems, and Next-Generation Satellites XXI* (Vol. 10423, p. 104230G). International Society for Optics and Photonics.
 40. Li, B., Sang, J., & Chen, J. (2018). Achievable orbit determination and prediction accuracy using short-arc space-based observations of space debris. *Advances in Space Research*, 62(11), 3065-3077.
 41. Sokol, G., Kotlov, V., Khorischenko, O., Davydova, A., & Heti, K. (2017, April). Using Spacecraft in Climate and Natural Disasters Registration. In *EGU General Assembly Conference Abstracts* (p. 8691).
 42. Cutter, M., Davies, P., Baker, A., & Sweeting, M. (2007, July). A high performance EO small satellite platform & optical sensor suite. In *2007 IEEE International Geoscience and Remote Sensing Symposium* (pp. 3851-3854). IEEE.
 43. Cawthorne, A., Beard, M., Carrel, A., Richardson, G., & Lawal, A. (2008). Launching 2009: The NigeriaSat-2 mission—High-performance Earth observation with a small satellite.
 44. Chizea, F. D. (2017). *Construction of X/S Band for Nigeriasat-2 Mission Control Centre and Validation of Data From the Satellite* (Doctoral dissertation).
 45. Ayantunji, B., Mai-Unguwa, H., & Halidu, I. (2014). Investigation of the Effects of Local Meteorology on L and S Band signal in Tropical Environment along a Slant Path: A case Study of Nigeria Sat 2. *40th COSPAR Scientific Assembly*, 40, A1-1.